Journal of Transportation Technologies, 2020, 10, 21-49
https://www.scirp.org/journal/jtts
ISSN Online: 2160-0481
ISSN Print: 2160-0473

Generation and Analysis of Hybrid-Electric Vehicle Transmission Shift Schedules with a Torque Split Algorithm

Nicholas J. Connelly, Derek I. George, Andrew C. Nix, W. Scott Wayne

West Virginia University, Morgantown, WV, USA
Email: nick.connelly151@gmail.com, derek.ivan.george2@gmail.com, Andrew.Nix.mail.wvu.edu, scott.wayne.mail.wvu.edu

How to cite this paper: Connelly, N.J., George, D.I., Nix, A.C. and Wayne, W.S. (2020) Generation and Analysis of Hybrid-Electric Vehicle Transmission Shift Schedules with a Torque Split Algorithm. *Journal of Transportation Technologies*, **10**, 21-49.
https://doi.org/10.4236/jtts.2020.101003

Received: December 13, 2019
Accepted: January 4, 2020
Published: January 7, 2020

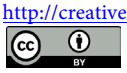

Abstract

The increased concern over global climate change and lack of long-term sustainability of fossil fuels in the projected future has prompted further research into advanced alternative fuel vehicles to reduce vehicle emissions and fuel consumption. One of the primary advanced vehicle research areas involves electrification and hybridization of vehicles. As hybrid-electric vehicle technology has advanced, so has the need for more innovative control schemes for hybrid vehicles, including the development and optimization of hybrid powertrain transmission shift schedules. The hybrid shift schedule works in tandem with a cost function-based torque split algorithm that dynamically determines the optimal torque command for the electric motor and engine. The focus of this work is to develop and analyze the benefits and limitations of two different shift schedules for a position-3 (P3) parallel hybrid-electric vehicle. a traditional two-parameter shift schedule that operates as a function of vehicle accelerator position and vehicle speed (state of charge (SOC) independent shift schedule), and a three-parameter shift schedule that also adapts to fluctuations in the state of charge of the high voltage batteries (SOC dependent shift schedule). The shift schedules were generated using an exhaustive search coupled with a fitness function to evaluate all possible vehicle operating points. The generated shift schedules were then tested in the software-in-the-loop (SIL) environment and the vehicle-in-the-loop (VIL) environment and compared to each other, as well as to the stock 8L45 8-speed transmission shift schedule. The results show that both generated shift schedules improved upon the stock transmission shift schedule used in the hybrid powertrain comparing component efficiency, vehicle efficiency, engine fuel economy, and vehicle fuel economy.

Keywords

Hybrid-Electric Vehicles, Torque Split Algorithm, Shift Schedule, Shift Map, Cost Function, SOC Dependent

1. Introduction

The effort to reduce tailpipe emissions from transport vehicles has grown in recent years. One area of improvement has been the effort to electrify vehicles to varying degrees, including development of mild-hybrid systems to fully electrified battery electric vehicles (BEV). Given currently available hardware, hybrid electric vehicles (HEV) offer advantages over both the internal combustion engine (ICE) and BEV architectures. The HEV has the potential to increase fuel economy and reduce emissions compared to an ICE vehicle, and improve range compared to a BEV with comparable cost.

To successfully operate HEVs, which are powered by two independent energy sources, a control strategy to split power usage from both powertrains is required. The reasons for developing a control strategy include controlling the state of charge (SOC) of the high voltage battery in order to maintain consistent power availability to the wheels for the driver and to optimize the consumption of energy and reduce production of tailpipe emissions, but are not limited to these constraints.

Various approaches have been applied to the development of control strategies, which tend to focus on the torque split between the engine and electric motor(s). To simplify the problem, and due to drive quality constraints, the transmission shift schedule is often set as static. A common practice is to use a look-up table that is a function of both accelerator pedal percentage (APP) and vehicle speed. Proposed is the addition of battery SOC, which would allow for the standard static look-up table approach, but also may allow the shift schedule to be calibrated more to fit the torque selection algorithm.

2. Hybrid Torque Split Algorithm

The hybrid torque split algorithm is comprised of two components: a shift schedule and a torque selection algorithm. The shift schedule is separated from the torque selection algorithm, because the shift schedule is determined offline, while the torque selection is performed online, during vehicle operation and control. Determination of the shift schedule offline allows the torque split algorithm to be less computationally intensive. A full description of both the shift schedule and torque selection algorithm in the current work and from previous literature is presented below.

2.1. Torque Split Algorithm

In recent years, significant work has been performed to optimize the selection of torque distribution in a hybrid-electric vehicle (HEV). Both the development of the Equivalent Consumption Minimization Strategy (ECMS) algorithm and use of Pontryagin's Minimum Principle (PMP) have been employed to optimize torque selection in HEVs [1]. The ECMS algorithm operates by minimizing a cost function, which equates electrical and conventional energy consumption.

The ECMS minimization function is shown Equation (1), below:

$$\dot{m}_{f,eqv}(t) = \dot{m}_f(t) + \frac{s(t)}{Q_{lhv}} * P_{batt}(t) * p(SOC) \tag{1}$$

where $\dot{m}_{f,eqv}(t)$ is the equivalent fuel consumption over time, $\dot{m}_f(t)$ is the fuel consumption over time, $s(t)$ is the equivalence factor, Q_{lhv} is the lower heating value of the fuel, $P_{batt}(t)$ is the power consumption by the electric powertrain and $p(SOC)$ is a penalty function to keep the SOC within tolerable limits [1]. The equation for $p(SOC)$ is presented below:

$$p(SOC) = \left(1 - \left[\frac{SOC(t) - SOC_{target}}{(SOC_{max} - SOC_{min})/2}\right]^a\right) \tag{2}$$

where $SOC(t)$ is the current battery SOC, SOC_{target} is the target battery SOC, SOC_{max} is the maximum battery SOC, SOC_{min} is the minimum battery SOC, and a is an exponential variable term.

Fu, *et al.* [2] demonstrated that the ECMS algorithm requires "accurate prior knowledge of the full trip and a trial-and-error search for the optimal equivalence factor". To avoid the shortcomings of the ECMS algorithm, an adaptive algorithm must be developed. Musardo [3] demonstrates an adaptive ECMS algorithm which adapts the equivalence factor based on the "past and predicted vehicle speed and GPS data" and is shown to produce a slightly suboptimal result. Furthermore, adaptive (A-ECMS) algorithms have been improved through application of Vehicle-to-Vehicle (V2V) and Vehicle-to-Infrastructure (V2I) information. Kazemi *et al.* [4] implemented both a standard A-ECMS algorithm as well as a modified A-ECMS algorithm, which updated the equivalence factor (EF) given information available via V2V and V2I networks in a parallel HEV. The authors showed a 2.4% fuel economy improvement over the conventional A-ECMS algorithm. Kazemi *et al.* [5] further developed adaptations to the A-ECMS for use in a parallel HEV and assessed the prediction window size and the effects it had on the EF and resulting improvements over the A-ECMS. The study concluded that future investigation would be required but found that a prediction window larger than 15 s started to degrade performance.

The torque selection algorithm studied in the current work is similar in nature to the ECMS algorithm, with a cost function that includes engine and motor power loss cost, a charge sustaining (CS) cost, and an engine torque transient cost. The equation for the cost function is as follows:

$$P_{Loss} = W_1 * P_{Loss,EV} + W_2 * P_{Loss,IC} + W_3 * P_{Loss,CS} + W_4 * P_{Loss,Trns} \tag{3}$$

where P_{Loss} is the final cost value, $P_{Loss,EV}$ is the power loss associated with the high-voltage (HV) battery, electric motor (EM) and inverter, $P_{Loss,IC}$ is the power loss associated with the internal combustion (IC) engine, $P_{Loss,CS}$ is a charge sustaining cost, $P_{Loss,Trns}$ is a factor applied to dampen transient engine

torque selections from the cost function, and W_1 through W_4 are weights that are calibrated to condition the function.

The $P_{Loss,EV}$ cost was determined off-line as a function of EM torque and speed according to the following equation:

$$P_{Loss,EV} = \left| I_{Batt} V_{Batt} - \tau_{Mot} * \omega_{Mot} \right| + \left[I_{Batt}^2 * R_{Batt} \right] \tag{4}$$

where I_{Batt} is the HV battery current, V_{Batt} is the HV battery voltage, τ_{Mot} is the EM torque, ω_{Mot} is the EM speed, and R_{Batt} is the HV battery resistance. To determine the values in the equation an equivalent circuit model and several equations were used, and the HV battery resistance and open-circuit voltage were first assumed as a constant value, by averaging them in the look-up table data supplied for each. From the equivalence circuit the following equation was derived:

$$V = I * R + OCV$$

where V represents the HV battery voltage, I is the current being drawn from the HV battery, R is the internal HV battery resistance determined from the lookup tables provided, and OCV is the open circuit voltage (OCV). Additionally, the following equations for the charge and discharge current were used:

$$Charge\ I = \frac{\tau * \omega}{V} \eta \tag{5}$$

$$Discharge\ I = \frac{\tau * \omega}{V} \frac{1}{\eta} \tag{6}$$

I represents the current drawn from the HV battery to operate the EM, τ is the torque output by the EM, ω is the EM's angular speed, V is the voltage input to the inverter, and η is the system efficiency. The same efficiency data is used for both charge and discharge current. The efficiency lookup table data accounts for rotor iron losses, other rotor losses, stator iron losses, moving losses and winding losses (I^2R).

The $P_{Loss,IC}$ power loss was determined off-line as a function of engine torque and speed. This was done using engine data taken from a MathWorks® Simulink model of the engine. The engine efficiency, torque and speed were used to find the power loss at each of the torque and speed points. These values were then renormalized by subtracting the power loss at the point of maximum efficiency from all points and taking the absolute value of these, according to the following equation:

$$P_{Loss,IC} = \left| P_{Loss,Map,IC} - P_{Loss,Eff,IC} \right| \tag{7}$$

where $P_{Loss,Map,IC}$ is the raw power loss calculated and $P_{Loss,Eff,IC}$ is the power loss at the most efficient point of the engine. The purpose of the normalization was to incentivize efficient operation of the engine during over the road charging operation. The normalization incentivizes efficient charging by putting the most efficient engine operating points as the lowest cost in the engine power loss

model table.

The $P_{Loss,IC}$ and $P_{Loss,EV}$ values are tabulated in lookup tables, normalized by the maximum power loss of each. The $P_{Loss,CS}$ term, which does not represent actual power loss, was developed to be a calibratable means of sustaining charge and is shown in the following equation:

$$P_{Loss,CS} = \left(\left(SOC_{Curr} - SOC_{Target}\right) * K_{Norm}\right)^{K_{Exp}} * \left(\frac{\tau_{mot,Pos}}{\tau_{mot,max}}\right) \quad (8)$$

where SOC_{Curr} is the current SOC of the HV battery, SOC_{Target} is the target SOC for the HV battery, K_{Norm} is a normalization term to set the upper and lower bounds of HV battery SOC, K_{Exp} is an exponential term to create a region of lesser influence closer to the HV battery target SOC in the form of a sigmoid function, $\tau_{Mot,Pos}$ is the EM torque value being evaluated, and $\tau_{Mot,Max}$ is the maximum possible EM torque.

The $P_{Loss,CS}$ term detailed above was inspired from the penalty function implemented in [1]. The primary difference in the implementation of both Equation (1) and Equation (3) is an additive approach in Equation (1) and a multiplicative approach in Equation (3) for the charge sustaining control. To supplement the additive nature of the applied power loss function the $\left(\tau_{mot,Pos}/\tau_{mot,max}\right)$ term was used to weigh each torque value based on the degree to which it is a negative torque, and therefore the degree it would produce charging current to the battery relative to the other torque values evaluated. Additionally, the normalization factor, K_{Norm} was used as a lumped calibration variable, as opposed to the $s(t)/Q_{lhv}$ term, which is comprised of the equivalence factor and the lower heating value of the fuel.

$P_{Loss,Trns}$ is also not a term representing actual power loss. It was proposed that the engine torque transient cost adds cost around the current engine operating point and thus for the $P_{Loss,Trns}$ term the following equation was developed to be calculated online (during vehicle operation):

$$P_{Loss,Trns} = \left(Sat\left(\tau_{Eng,pos} - \tau_{Fdbk}\right) * K_{Norm}\right)^2 \quad (9)$$

where $\tau_{Eng,Pos}$ is the potential engine operating point being evaluated, τ_{Fdbk} is the current engine torque command, *Sat* is a saturation applied within calibratable bounds deemed K_{Sat}, and K_{Norm} is a calibratable normalization applied. A diagram of the parameters and the impacts they have on the cost is shown in **Figure 1**.

2.2. Shift Schedule

Overall vehicle efficiency is also dependent on the current transmission gear at a given speed and torque input to the transmission simply because it affects the power output (and losses) from the engine to the wheels. To utilize the torque split algorithm to its full potential, two transmission shift schedules were investigated:

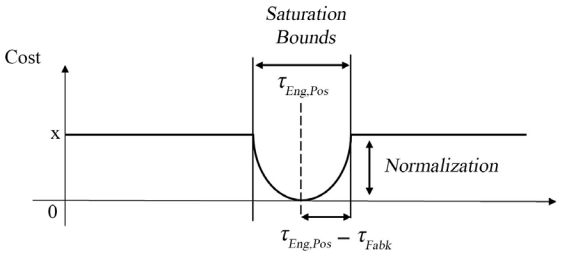

Figure 1. Torque split algorithm cost function.

- An optimized two-parameter shift schedule, or SOC independent shift schedule (represented in **Figure 2**)
- An optimized three-parameter shift schedule, or SOC dependent shift schedule (represented in **Figure 3**), that adapts to fluctuations in SOC of the high voltage batteries

The goal of the hybrid shift schedules is to determine the optimal gear for the transmission for the current vehicle state to improve fuel economy and reduce energy consumption of a plug-in parallel hybrid-electric vehicle by increasing overall vehicle efficiency and reducing engine fuel consumption compared to the stock 8-speed 8L45 transmission shift schedule designed for a 2016 Chevrolet Camaro. The overall vehicle performance is generally defined by the following two aspects:

- Overall vehicle efficiency: The overall efficiency of the power flow of the ICE powertrain and electric powertrain to the wheels. By focusing on overall vehicle efficiency, high voltage battery discharging and charging events are optimized subsequently increasing the vehicle's overall fuel economy.
- Engine fuel consumption: Fuel energy consumption by the engine. This metric was chosen because the power loss of the engine greatly outweighs the power loss of the electric powertrain by approximately a factor of 10. A typical ICE engine (30% to 40% efficiency) is much more inefficient than an electric motor (60% to 98% efficiency). Additionally, the energy density of a carbon-based fuel is much higher than that of electric energy storage. The lower efficiency of an engine coupled with the high energy density of carbon-based fuel results in massive power losses in ICE powertrains. Focusing on lowering engine fuel consumption will have a great impact on the overall vehicle's energy consumption and will reduce the pump-to-wheel emissions.

Shift schedules were generated through an exhaustive search method coupled with a fitness function to analyze how "fit" each transmission gear was for all valid vehicle operating points. Once generated, a sensitivity analysis was performed to quantify the impact of the generated shift schedule that adapts to fluctuations in SOC of the HV batteries, or SOC dependent shift schedule, versus the generated traditional static shift schedule, or SOC independent shift schedule.

The generated shift schedules are a function of the driver's accelerator pedal position, or APP, and vehicle speed. Shift schedules consist of gear threshold shift lines, which indicated when the transmission would perform either an upshift or a downshift. Where the two valid ranges overlap results in the overall

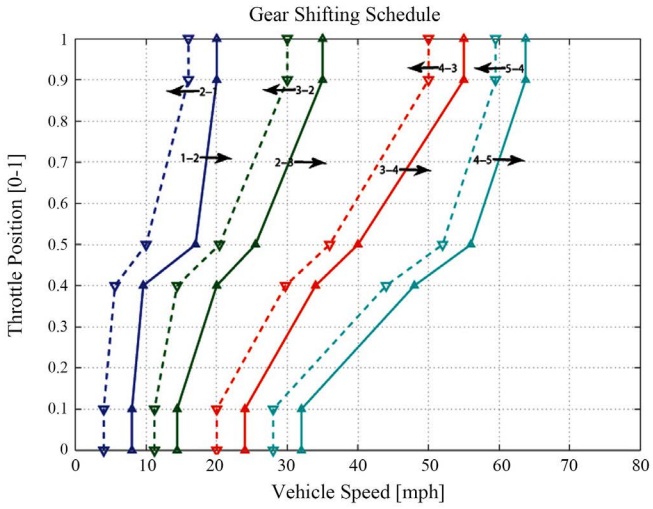

Figure 2. General two-parameter shift schedule representation [6].

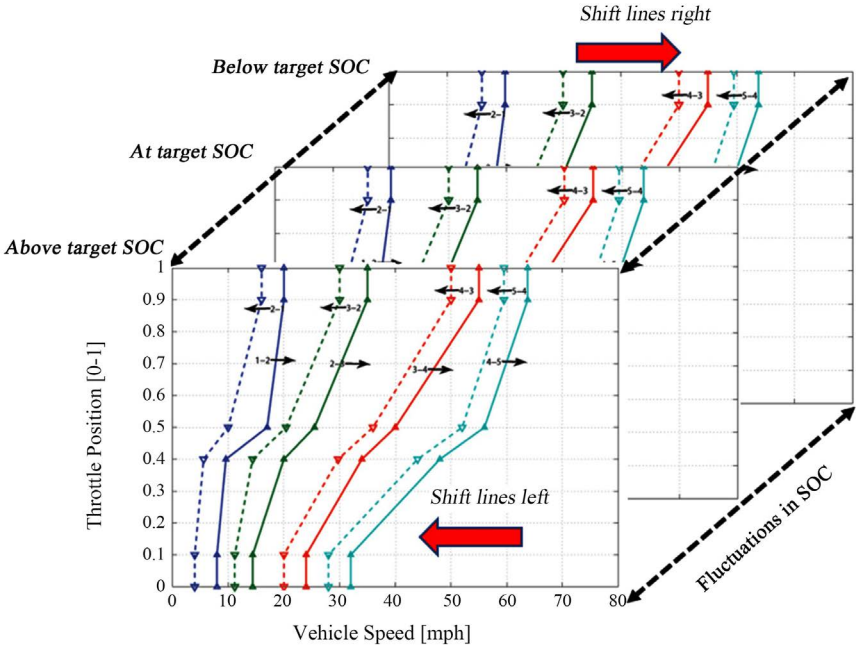

Figure 3. General three-parameter shift schedule representation.

operating point validity. This process is outlined in Equation (10) where $V_{O,i,j,k}$ is the overall gear validity, $V_{T,i,j,k}$ is the torque validity, $V_{S,i,j,k}$ is the speed validity, $T_{D,i,j}$ is the driver torque demand, $T_{M\,Max,i}$ is the max motor torque, $N_{Veh,i}$ is the vehicle speed, $N_{E,i,k}$ is the engine speed, $N_{E,Max}$ and $N_{E,Min}$ are the maximum and minimum engine speeds allowed for the engine respectively, $G_{Rat,k}$ is the gear ratio, and the subscripts *i*, *j*, and *k* are the current vehicle speed state, current accelerator pedal position, and current transmission gear respectively.

$$\begin{aligned} V_{O,i,j,k} = & \left[V_{T,i,j,k} \left(T_{D,i,j,}, T_{M,Max,?}, G_{Rat,k} \right) \right] \\ & \cup \left[V_{S,i,j,k} \left(N_{Veh,i}, N_{E,i,k}, N_{E,Max}, N_{E,Min}, G_{Rat,k} \right) \right] \end{aligned} \tag{10}$$

The fitness of the viable operating points is then calculated to obtain the optimal gear for the current vehicle state. Since the vehicle in this study has a parallel (P3) hybrid architecture and only the engine is directly affected by the transmission, the fitness is defined as a function of engine power loss and engine efficiency at the current operating point. This definition will result in the engine operating in a torque vs. speed curve region that will allow the torque selection algorithm to select a torque that will operate the engine as efficiently as possible. Equation (11) shows the fitness function used where $\eta_{E,i,j,k}$ is engine efficiency, $PL_{E,i,j,k}$ is the engine power loss, $PL_{E,Max}$ is the maximum engine power loss, and W_η and W_{PL} are the associated weighting coefficients.

$$F_{i,j,k} = W_\eta * \eta_{E,i,j,k} + W_{PL} * \left(1 - \frac{PL_{E,i,j,k}}{PL_{E,Max}}\right) \tag{11}$$

The gear that achieves the highest fitness for that operating point will generate the optimal shift lines for the vehicle. Equation (12) calculates the resulting optimal shift lines where $G_{Map,i,j}$ is the optimal two-parameter shift schedule for the vehicle as a function of accelerator pedal and vehicle speed (**Figure 4**) where the solid lines represent upshift lines and the dashed lines represent downshift lines. If the current vehicle operation point (accelerator pedal position and vehicle speed) crosses an upshift line from the left, an upshift is command. The inverse is true for the downshift lines.

$$G_{Map,i,j} = max_k \left(F_{i,j,k}\right) \tag{12}$$

The three-parameter shift schedule was generated by assuming a minimum amperage rate as a function of deviation away from the target SOC and the two-parameter shift map. A fixed amperage rate defines the minimum amount of charging (or discharging) torque required for the current SOC, which in turn defines the amount of engine torque needed to meet the driver torque demand. A calibratable sigmoidal function of the minimum amperage rate as a function of SOC was initially chosen to avoid abrupt gear shifts if the SOC deviation was small (**Figure 5**). In the charging region (below target SOC), if the current gear ratio is not able to allow the engine to meet the required torque demand the gear ratio is increased, or a downshift occurs. The opposite is true for the discharging region.

3. Testing Environments

The completion of the shift schedule implementation led to testing in the software-in-the-loop (SIL) environment and vehicle-in-the-loop (VIL) environment using the same drive cycle. The shift schedules were tested on two back-to-back cycles of the AVTC EcoCAR 3 competition emissions and energy consumption (E&EC) drive cycle shown in **Figure 6**. The E&EC drive cycle consists of a weighted sum of four EPA standard drive cycles: UDDS 505 (29%), HWFET (12%), US06 City (14%), and US06 Highway (45%). The cycle is approximately 28 miles and takes approximately 42 minutes to complete in real-time.

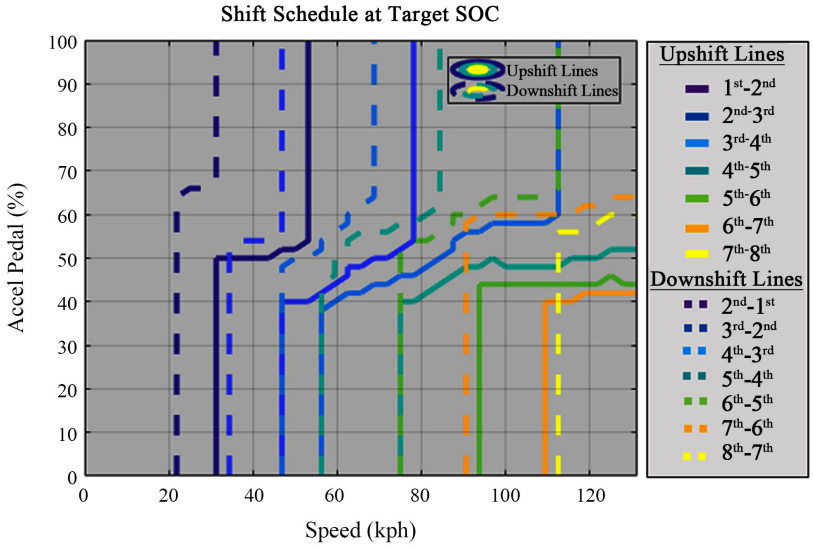

Figure 4. Shift schedule at target SOC.

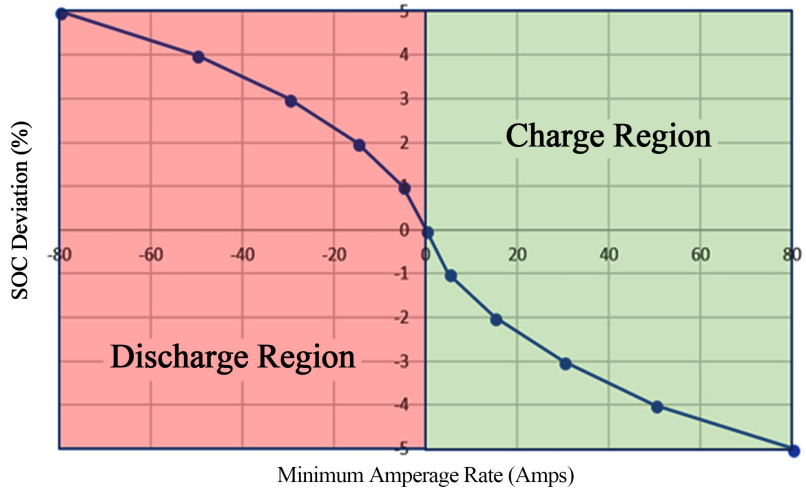

Figure 5. Initial sigmoidal function of SOC deviation vs. minimum amperage rate.

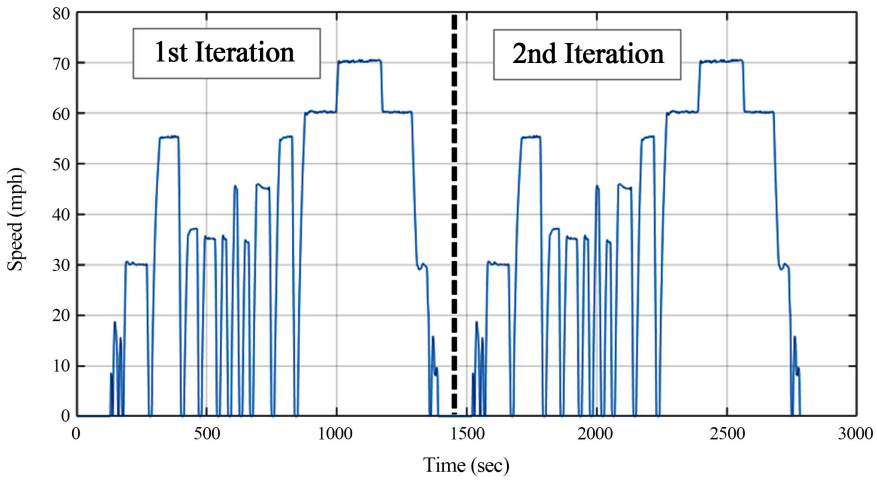

Figure 6. E&EC drive cycle—2 iterations.

3.1. Software-in-the-Loop (SIL) Environment

Software-in-the-loop (SIL) simulations were performed with a full vehicle model of the hybrid-electric vehicle developed in MATLAB/Simulink. The model consists of three main systems: a Vehicle System, a Driver System, and a Controller System.

The Vehicle System is a Simulink model created to represent the vehicle and utilizes the Simscape toolboxes provided in MATLAB/Simulink to simulate physical connections of the rotational masses within the drivetrain (driveshaft, rear differential, transmission, engine, wheels, etc.). This system also models the communication interfaces between the primary electronic control modules, or ECMs, within the vehicle and simulates their behavior.

The Driver System is a Simulink model created to simulate a driver. This system oversees simulating startup and shutdown of the vehicle, accelerator pedal input (APP) input, brake pedal input, and park-reverse-neutral-drive-manual (PRNDM) shifting into the Controller System and is the driving force of the three systems.

The Controller System houses the supervisory control algorithm for the vehicle. This system is where all hybridization control algorithms for the vehicle were developed. From a high-level perspective, this algorithm mainly consists of the gear request logic (GRL), which contains the hybrid shift schedules and torque split algorithm (TSA) seen in **Figure 7**.

3.2. Vehicle-in-the-Loop (VIL) Environment

Vehicle testing was performed using the light-duty chassis dynamometer test cell in the Vehicle Emissions Testing Laboratory (VETL) at the WVU Center for Alternative Fuels, Engines and Emissions (CAFEE). The facility is comprised of a Title 40 CFR, Part 1066-compliant [7] Horiba® 4WD Vulcan II emission chassis dynamometer with an accompanying Title 40 CFR, Part 1065 [8] compliant constant volume sampling (CVS) emissions sampling system for spark-ignited and compression-ignited engine vehicles, as well as hybrid, plug-in hybrid and electric vehicles [9]. The dual-roller dynamometer can accommodate testing of two-, four- and all-wheel drive vehicles.

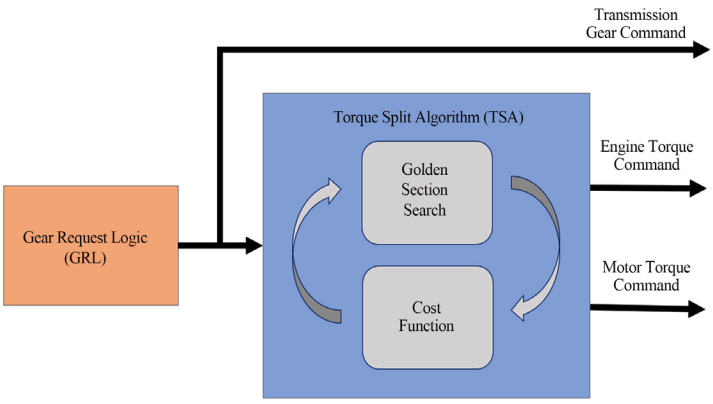

Figure 7. Controller system high-level flow chart.

The fuel economy results were calculated using equations based on the Society of Automotive Engineers (SAE) J1711 guidelines [10]. The energy consumed by each torque producing powertrain component was first calculated. The electric energy consumed by the electric motor in Wh/km was calculated by analyzing the change between the initial SOC and final SOC of the energy storage system (ESS) over a drive cycle to find the amount of battery pack energy lost in Ah. This value is then multiplied by the nominal pack voltage of 340 volts and divided by the total distanced traveled to find the ESS energy used per kilometer (Wh/km), as shown in Equation (13), where EC_{ESS} is the ESS electric energy consumed and $ESS_{Peak\ Cap}$ is the ESS peak pack capacity (39.2 Ah).

$$EC_{ESS} = \left(\frac{Initial\ SOC - Final\ SOC}{100}\right) * ESS_{Peak\ Cap} * 340\ \text{V} * \frac{1}{Distance\ Traveled} \tag{13}$$

The fuel energy consumed was calculated by taking the product of the total volume of fuel consumed over the drive cycle in grams and multiplying by the specific energy density of the fuel used (fuel density of E85 is 7.85 Wh/g [11] and dividing by the distanced traveled to obtain the fuel energy consumption per kilometer. Equation (14) outlines this process where EC_{Fuel} is the fuel energy consumed.

$$EC_{Fuel\ E85} = \frac{Fuel\ Consumed\ of\ E85 * 7.85\ \text{Wh/g}}{Distance\ Traveled} \tag{14}$$

Because this is a hybrid-electric vehicle capable of sustaining battery SOC with engine power, a correction factor is then applied to the fuel energy consumed to account for the conversion of fuel energy to electric energy or charging events. This was done by taking the sum of the fuel energy consumed and the electric energy consumed applied with a conversion factor. The conversion factor used in this analysis is 0.25 as it is the standard for SAE J1711 [10]. This process is outlined in Equation (15) where $EC_{Fuel,SOC\ corrected}$ is the SOC corrected fuel energy consumed.

$$EC_{Fuel\ E85,SOC\ corrected} = EC_{Fuel} + EC_{ESS} * 0.25 \tag{15}$$

The total energy consumption is then found by adding the SOC corrected fuel energy consumed and the ESS electric energy consumed. The vehicle fuel economy in mpgge is then found through Equation (16) where LHV_{E10} is the lower heating value of E10, or gasoline, in Wh/gal [12].

$$FE_{Veh} = \frac{1}{EC_{Fuel\ E85,SOC\ corrected} + EC_{ESS}} * LHV_{E10} \tag{16}$$

The fuel economy of the engine in mpg was calculated from instantaneous fuel flow reported over CAN from the ECM by simply dividing the total miles traveled when the engine was on by the integration of the instantaneous fuel flow converted to gallons per second. Equation (17) shows the engine fuel economy calculation from fuel flow data where $FE_{Eng,Inst\ FF}$ is the engine fuel

economy from instantaneous fuel flow.

$$FE_{Eng,Inst\ FF} = \frac{Distance\ Traveled}{\int Instantaneous\ Fuel\ Flow\ of\ E85} \quad (17)$$

A carbon balance was performed to verifiy the engine's fuel efficiency calculation in Equation (17), but emissions were not the primary focus. Equation (18) [13] outlines the carbon balance equation used where $FE_{Eng,CB}$ is the fuel economy of the engine from carbon balance, C_{HC} is the amount of HC emitted in grams, C_{CO} is the amount of CO emitted in grams, C_{CO2} is the amount of CO_2 emitted in grams, and FCC_{E85} is the fuel carbon content of E85 ethanol. Emissions data for this calculation was taken at VETL.

$$FE_{Eng,CB} = \left(\frac{\left(\left(0.817 * C_{HC} \right) + \left(0.429 * C_{CO} \right) + \left(0.273 * C_{CO2} \right) \right)}{Distance\ Traveled} \right)^{-1} * FCC_{E85} \quad (18)$$

4. Results

4.1. Resultant Shift Schedules

The procedures detailed in Section 2.2 were carried out and yielding the resultant SOC independent shift schedule is shown in **Figure 8**. The path each shift line takes follows the "s-shaped" trend of a generic shift schedule. At lower speeds and low APP, each line starts low and to the left. As either speed, APP, or both increase, the line starts to shift up and to the right creating the traditional "s-shape". If APP is held constant at 0%, or no driver accelerator pedal input (zero pedal), and the vehicle is increasing in speed, the shift schedule commands upshifts much sooner to decrease the torque capacity of the engine at the wheels. The engine torque capacity is decreased because less engine torque is needed to meet demand. Inversely, if APP is held constant at 100%, or wide-open throttle (WOT), upshifts occur much later to increase the torque capacity of the engine at the wheels longer to maximize the torque produced. The final resolution of this shift schedule is a 51 × 43 matrix with 2193 possible vehicle operating points where: APP = 0% to 100% in steps of 2% (51 steps) and vehicle speed = 0 to 131.25 kph in steps 3.125 kph (43 steps).

The resultant SOC dependent shift schedule is illustrated by the change in the upshift lines and downshift lines 5% above and 5% below the target SOC in **Figure 9** and **Figure 10**. The dotted lines represent the upshift/downshift lines at the target SOC, while the solid lines represent the deviated shift line. The shift schedule thresholds have moved further to the right and down as SOC deviates further below the target SOC and the shift schedule thresholds moving further to the left and up as SOC deviates further above the target SOC. The final resolution of this shift schedule is a 51 × 43 × 7 matrix with 15,351 possible vehicle operating points where: APP = 0% to 100% in steps of 2% (51 steps), vehicle speed = 0 to 131.25 kph in steps 3.125 kph (43 steps), and SOC = 30% to 40% in a variable step range of 30%, 32%, 34%, 35%, 36%, 38%, and 40% (7 steps). The SOC dependent shift schedule in its entirety is shown in Appendix A.

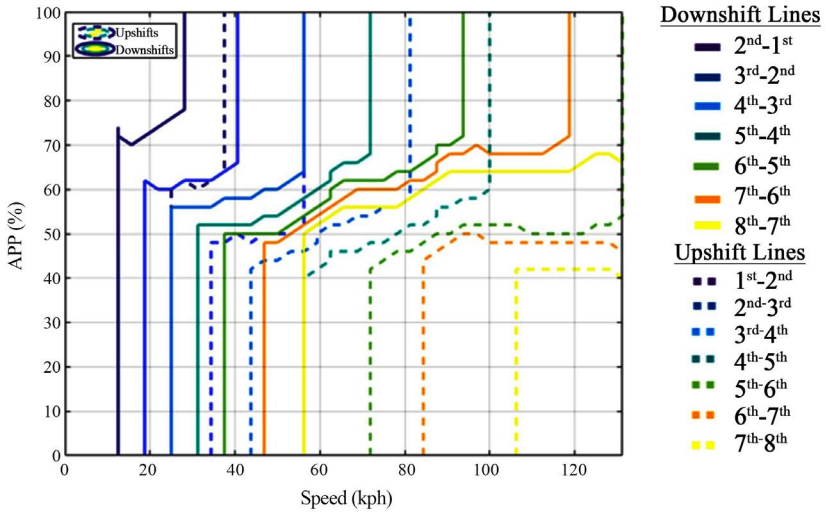

Figure 8. SOC independent shift schedule.

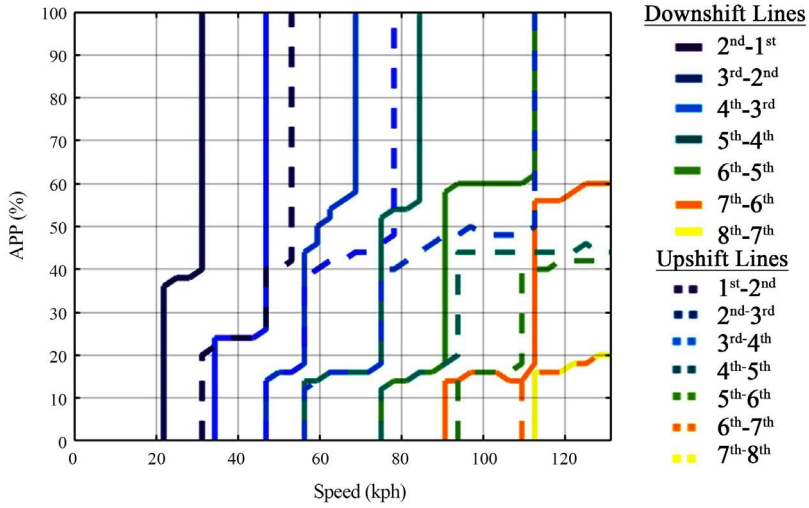

Figure 9. Shift schedule 5% below target SOC of SOC dependent shift schedule.

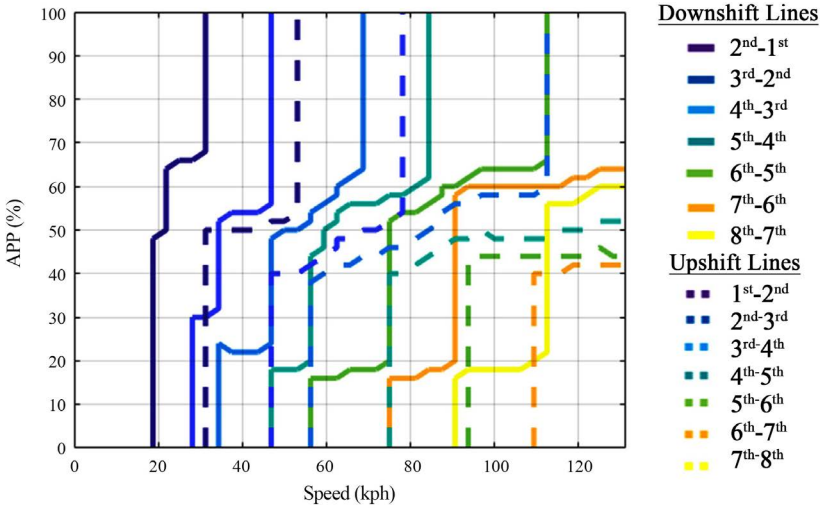

Figure 10. Shift schedule 5% above target SOC of SOC dependent shift schedule.

4.2. Software-in-the-Loop (SIL) Results

The vehicle operating mode for the SIL tests was charge sustaining (CS) mode and the charge depleting (CD) mode of the plug-in hybrid vehicle is not considered in the analysis, as the engine and transmission are not operating in CD mode. The fuel economy and efficiency results for the SOC independent shift schedule and SOC dependent shift schedule with an initial SOC of 35% (the target SOC) are shown in Table 1. Due to lack of access to the 8L45 transmission source code, no SIL results could be obtained for the transmission stock shift schedule. The percentage difference of the efficiency and fuel economy results from both shift schedules were calculated using the SOC independent data as a reference. This was done because the results are virtually identical in the SIL environment.

The percentage difference between the two shift schedules favored the SOC dependent shift schedule as it performed slightly better than the SOC independent in all categories. The SOC dependent shift schedule has higher engine and vehicle fuel economies and a higher component efficiency over two iterations of the E&EC drive cycle. However, the differences are small and within uncertainty estimates such that the SOC dependent shift schedule has no apparent significant advantages over the SOC independent shift schedule. This is most likely due to the starting point of the initial SOC being the target SOC for the control algorithm. As previously discussed, the SOC dependent shift schedule is identical to the SOC independent shift schedule at the target SOC due to the method used to generate the shift schedules. If the SOC did not deviate from the target over the drive cycle very far, the alterations in the SOC dependent shift schedule's shift lines would not be significant.

Table 1. SIL fuel economy and efficiency.

		Shift Schedule Used		
Parameter	Unit	SOC Independent	SOC Dependent	Percent Difference
Initial SOC	%	35	35	0.00%
Final SOC	%	36.7	36.5	−0.55%
Engine Fuel Economy	mpg	17.3	17.4	+0.57%
Engine Efficiency [Equation (17)]	%	28.6	28.7	+0.35%
Motor Discharge Efficiency	%	62.6	63.1	+0.79%
Motor Charge Efficiency	%	75.5	75.9	+0.53%
Vehicle Fuel Economy [Equation (16)]	mpgge	23.8	24.0	+0.83%
Vehicle Efficiency	%	38.0	38.0	0.00%

4.3. Vehicle-in-the-Loop (VIL) Results

Similar to SIL testing, the vehicle operating mode for the VIL tests was charge sustaining mode and the charge depleting mode of the vehicle is not considered in the analysis. The VIL results were gathered from fuel economy and emissions testing on the light duty chassis dynamometer test cell at the CAFEE VETL located in Morgantown, West Virginia. The emissions data was collected from the CAFEE Horiba described in Section 3.2, while the instantaneous vehicle information was collected from the vehicle's controller area network (CAN). The fuel economy and efficiency results for the SOC independent shift schedule, SOC dependent shift schedule, and stock transmission shift schedule are shown in Table 2 for the EcoCAR competition test cycle. It should be noted that the engine efficiency, vehicle fuel economy, and vehicle efficiency values for all shift schedules have increased from the SIL environment. This is due in part to inaccurately modeled drivetrain parasitic losses within the full vehicle model in the SIL environment.

An example is the modeled drivetrain patristic losses of a Simscape torque converter between the modeled engine and transmission. The torque converter losses were added to the model in an attempt to increase the fidelity of the model to better represent the vehicle, but the system could not be properly calibrated from lack of understanding how the Simscape block functioned. The calibration of the torque converter was very rigid and sensitive, meaning a small change in the value within the block resulted in a massive change within the full vehicle model. Multiple components within the full vehicle model suffered from similar model sensitivity issues and due to lack of necessary on-road testing and time constraints the full vehicle model was not calibrated to appropriately simulate the losses of the real the vehicle. Subsequently, the losses seen in the full vehicle model were actually greater than that of the vehicle.

Table 2. VIL fuel economy and efficiency.

		Shift Schedule Used		
Parameter	Unit	SOC Independent	SOC Dependent	Stock Transmission
Initial SOC	%	38	38	38.5
Final SOC	%	38	38.5	38
Engine Fuel Economy [Equation (17)]	mpg	18.0	18.5	14.6
Engine Efficiency	%	35.8	36.1	33.7
Motor Discharge Efficiency	%	70.4	66.3	72.1
Motor Charge Efficiency	%	83.0	83.9	81.4
Vehicle Fuel Economy [Equation (16)]	mpgge	34.8	35.3	33.6
Vehicle Efficiency	%	48.0	47.9	47.7

Also, it was observed that during vehicle testing, the engine shut off periodically. This was due to the supervisory control algorithm deeming the SOC was too high. This behavior is illustrated in **Figure B1** in Appendix B at the points where the engine speed CAN signal goes to zero. A periodic engine shut down was not witnessed during the SIL testing and may be the main contributor to why the engine efficiency, vehicle fuel economy, and vehicle efficiency values have increased in the VIL environment. However, the correlation between the shift schedules in each environment is still practicable. Additional vehicle CAN data from VIL testing is shown in Appendix B. These results include engine speed, engine torque, fuel flow rate, SOC, vehicle speed, ESS current, ESS voltage, and transmission gear versus time as well as a summary table including and energy consumption and efficiency analysis.

In addition to calculating the engine fuel economy from the instantaneous fuel flow, the engine fuel economy was also calculated by carbon balance method, to permit a comparison between the two methods. The total emissions in grams from CO, CO_2, and HC as well as the distance traveled with the engine on and the total distance traveled are shown in **Table B1** in Appendix B. The SOC dependent shift schedule significantly reduced the amount of CO_2 emissions produced from both the SOC independent shift schedule by approximately 16% and the stock transmission shift schedule by approximately 7.5%. This indicated that the SOC dependent shift schedule allowed the high voltage batteries to charge more quickly allowing the engine to shut off sooner, resulting in less emissions produced over the cycle. Additional emissions data collected is shown in Appendix B.

The resulting engine fuel economy calculations from carbon balance and the deviation from the instantaneous fuel consumption engine fuel economy are shown in **Table 3**. The carbon balanced fuel economy 5% - 9% lower than the instantaneous fuel consumption fuel economy for all shift schedules apart from the SOC independent shift schedule. The SOC independent shift schedule carbon balance fuel economy shows 21.6% decrease compared to the instantaneous fuel consumption fuel economy.

Because the trend in fuel economy numbers of instantaneous fuel consumption from SIL to VIL are consistent and within the fuel flow uncertainty of 3% [14], it was suspected that there was an error in the modal emission data collected, namely the CO_2 emissions analyzer. However, upon inspection of the CO_2 emission rate and the percent error of the emission data analyzers [8], it was clear that the tailpipe continuous CO_2 emissions were higher during the SOC independent test than the SOC independent test as shown in **Figure B2** and **Figure B3** in Appendix B. **Figure B2** shows the continuous CO_2 emission rates of between the two tests and **Figure B3** shows the cumulative sum of the CO_2 emissions. The estimation of the percent error of the emissions data analyzers is impractical due to the number of independent sensors in the system and was not readily available. CAFEE uses the standard percent error of emissions data collection given by CFR Part 1065 [8] of approximately 2.24%.

Table 3. Engine fuel economy—instantaneous fuel consumption and carbon balance comparison.

Shift Schedule Used	Engine Fuel Economy (mpg)		
	Instantaneous Fuel Consumption [Equation (17)]	Carbon Balance [Equation (18)]	Percent Difference
SOC Independent	18.0	14.8	−21.6%
SOC Dependent	18.5	17.7	−4.5%
Stock Transmission	14.6	13.4	−9.0%

4.4. Sensitivity Analysis

To perform a more in-depth study of how the SOC dependent shift schedule impacts vehicle performance as the SOC changes, a sensitivity analysis was performed by changing the initial SOC of the simulation in the SIL environment to explore more of the shift schedule. Results were obtained from the vehicle model in the SIL environment at three different initial SOC settings while the target SOC was kept constant: 1) at 5% below the target SOC, 2) at 5% above the target SOC, and 3) at the target SOC. The control algorithm utilized a target SOC of 35%, leading to an SOC of 30% and 40% for the first and second cases above, respectively.

The resultant commanded gear from the SOC dependent shift schedule from each case over the drive cycle is shown in **Figure 11** with black representing an initial SOC of 35%, blue representing an initial SOC of 30%, and red indicating an initial SOC of 40%. Where the lines get clipped at the upper portion of the graph is where the transmission was in neutral and should be ignored.

As seen in **Figure 11**, no discernable difference can be seen between the commanded gears if the initial SOC is changed. However, there are subtle differences when zoomed in, notably towards the beginning of the simulation. **Figure 12** is a zoomed in image of **Figure 11** between times of 60 seconds and 220 seconds of the simulation indicated on **Figure 11** by *Area 1*. In this figure, the command gear at an initial SOC of 30% is more distinguishable from the gear commands at the initial SOC of 35%. When the initial SOC is set at 30%, the SOC dependent shift schedule upshifted later in the simulation during vehicle accelerations. Similarly, the SOC dependent shift schedule downshifted sooner during the vehicle decelerations. These trends coincide with the basic premise of the SOC dependent shift schedule when the SOC is below the target SOC; a lower gear supplies more engine torque to the wheels and to the high voltage batteries. However, this late upshifting and early downshifting only occurred at these three points in the beginning of the simulation.

Once the high voltage battery is charged enough to be above the target SOC, the SOC dependent shift schedule attempted to minimize the engine torque at the wheels to conserve fuel. However, no occurrences of this were found during SIL testing, indicating that the SOC dependent shift schedule's calibratable minimum amperage rates are too strict.

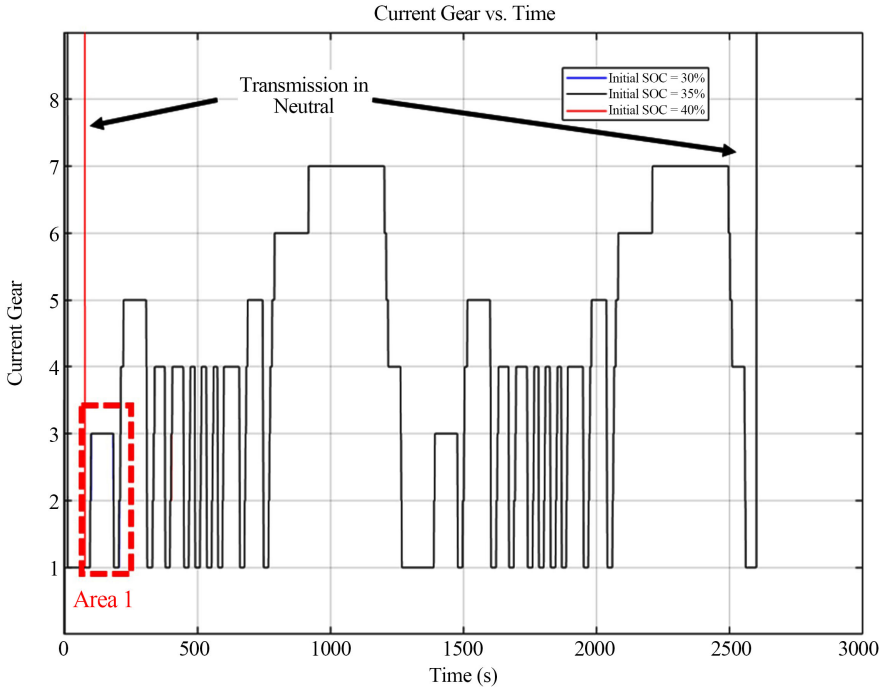

Figure 11. SOC dependent shift schedule gear commands with varying initial SOC.

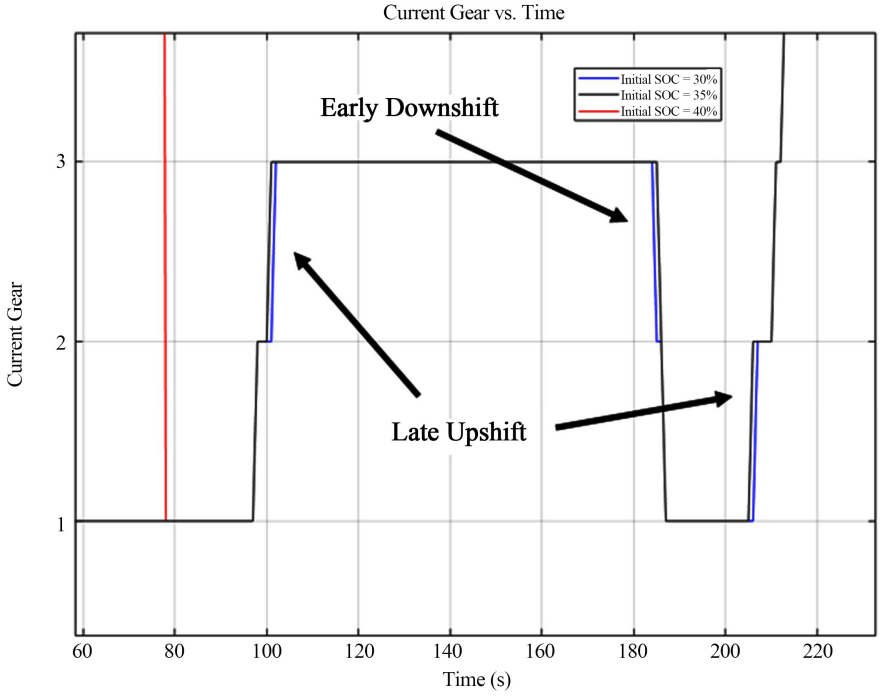

Figure 12. Commanded gear enhanced area 1.

The resultant trends of the final SOC, engine fuel economy, engine efficiency, motor discharging efficiency, motor charging efficiency, vehicle fuel economy, and vehicle efficiency are summarized in **Table C1** and **Table C2** and shown visually in **Figure C1** through **Figure C6** in Appendix C. The results show that the impact of varying the initial SOC with the SOC dependent shift schedule is

small because the shift schedule could not be used to its full potential. To explore more of the SOC dependent shift schedule, the initial SOC must be changed; this is in addition to varying the inputs of APP and vehicle speed, which can be done by varying drive cycles. This testing was not performed in the current work. However, some trends should be noted. The engine fuel economy, for example, has a slight upward trend as the initial SOC increases. This is primarily due to the basic concept within the supervisory control algorithm: if SOC is above the target SOC, the engine is used less and the electric motor more; if SOC is below the target SOC, use the engine more and the electric motor to charge. However, these trends could be a result of the torque split algorithm that was developed for the vehicle, rather than the transmission shift schedule [15]. These results include engine speed, engine torque, fuel flow rate, SOC, vehicle speed, ESS current, ESS voltage, and transmission gear versus time as well as a summary table including energy consumption and efficiency analysis.

4. Conclusions

The objective of this research was the generation and sensitivity analysis of two hybrid shift schedules for a transmission in a position 3 (P3) parallel hybrid-electric vehicle with the objectives of minimizing energy consumption and increasing vehicle fuel economy, while reducing emissions. The two shift schedules that were generated were a traditional two-parameter (SOC independent) shift schedule that operates as a function of the driver's accelerator position and the vehicle's speed, and a three-parameter shift schedule (SOC dependent shift schedule) that also adapts to fluctuations in the state of charge of the high voltage batteries.

To create the shift schedules, first, a gear validation was performed using vehicle torque capacity and vehicle speed as the boundary conditions. Then an exhaustive search was coupled with a fitness function to evaluate all possible vehicle operating points of the most "fit" gear for that operating point. The metrics used for evaluating the fitness included engine power loss and overall vehicle efficiency. The shift schedule generated from the maximum fitness evaluated for each vehicle operating point generated the two-parameter shift schedule, or SOC independent shift schedule. To create the SOC dependent shift schedule, the SOC independent shift schedule was used as the foundation for the target SOC. This foundation was altered based on a calibratable minimum amperage rate needed for a given SOC to modify the upshift and downshift lines of the SOC independent shift schedule, creating the SOC dependent shift schedule.

The shift schedules were then tested and analyzed in the software-in-the-loop (SIL) environment and vehicle-in-the-loop (VIL) environment. The results showed that both generated shift schedules improved the engine fuel economy, vehicle fuel economy, and overall vehicle energy consumption of the vehicle from the stock 8L45 automatic transmission shift schedule for a production 2016 Chevrolet Camaro. However, when the generated shift schedules were compared

to each other, neither demonstrated significant improvements over the other.

The sensitivity analysis performed on the SOC dependent shift schedule in the SIL environment consisted of running the EcoCAR 3 emissions and energy consumption (E&EC) drive cycle while varying the initial SOC from 30%, 35%, and 40%. The results indicated that the commanded gear from the SOC dependent shift schedule rarely varied in each case. At the beginning of the simulation during the initial SOC at 30% case was the only time a difference could be found within the SOC dependent shift schedule. After the torque split algorithm stabilized and sustained the target SOC, it was shown that SOC had little effect on the resultant shift schedule. The summary results for the sensitivity analysis yielded similar outcomings netting on average a 2% deviation as the initial SOC was varied. This is in part due to the lack of exploration of the SOC dependent shift schedule's full potential. In order to thoroughly analyze this shift schedule, testing with other EPA drive cycles with varying the initial SOC would be necessary.

While the results demonstrated that the SOC dependent shift schedule performed slightly better than the SOC independent shift schedule, the SOC dependent shift schedule will require more processing power during vehicle operation due to the 3-dimensional interpolation being performed. Because the hybrid supervisory controller, or HSC, used in the test vehicle has more processing power than a typical vehicle electronic control unit, or ECU, this issue was never experienced. The performance of these two shift schedules could be further investigated by comparing the processing overhead of the HSC over a drive cycle executed with each shift schedule. However, the indistinguishable differences between the two shift schedules warrant further investigation into the generation and calibration of the SOC dependent shift schedule.

Another recommendation is the optimization method of the shift schedule. The optimization method was a heuristic one of iterative SIL and VIL tests coupled with good engineering sense. This was done because the shift schedules also had to be generated and compared, to form a baseline measurement to determine which method was superior. Further optimization of the selected shift schedule could be more adequately performed through use of dynamic programming similar to the research done by Shen, *et al.* [16]. Based on the analyses performed, the SOC dependent shift schedule warrants further research to be optimized.

Acknowledgements

This work was performed under partial funding of graduate students by the EcoCAR 3 Advanced Vehicle Technology Competition, sponsored by US Department of Energy and General Motors (GM), and managed by Argonne National Laboratory. The authors would like to thank the WVU Center for Alternative Fuels, Engines and Emissions (CAFEE), specifically all of the workers who donated additional time to assist our team in emissions and fuel economy VIL testing. We very much appreciate the partnership between our team and CAFEE.

Thanks specifically to Aaron Barnett, Chris Rowe, Matt Cummings, Josh Matheny and CAFEE Director, Dan Carder. Also, a big thank you to our GM EcoCAR mentor, Dr. William Cawthorne, for his assistance with the entire torque split algorithm, as well as his support through the testing process.

Conflicts of Interest

The authors declare no conflicts of interest regarding the publication of this paper.

References

[1] Onori, S., Serrao, L. and Rizzoni, G. (2016) Hybrid Electric Vehicles Energy Management Strategies. Springer, London. https://doi.org/10.1007/978-1-4471-6781-5

[2] Fu, L., Ozguner, U., Tulpule, P. and Marano, V. (2011) Real-Time Energy Management and Sensitivity Study for Hybrid Electric Vehicles. *American Control Conference*, San Francisco, 29 June-1 July 2011, 2113-2118. https://doi.org/10.1109/ACC.2011.5991374

[3] Musardo, C., Rizzoni, G., Guezennec, Y. and Staccia, B. (2005) A-ECMS: An Adaptive Algorithm for Hybrid Electric Vehicle Energy Management. *European Journal of Control*, **11**, 509-524. https://doi.org/10.3166/ejc.11.509-524

[4] Kazemi, H., Khaki, B., Nix, A., Wayne, S. and Fallah, Y. (2015) Utilizing Situational Awareness for Efficient Control of Powertrain in Parallel Hybrid Electric Vehicles. *IEEE International Conference on Ubiquitous Wireless Broadband*, Montreal, 4-7 October 2015, 1-5. https://doi.org/10.1109/ICUWB.2015.7324524

[5] Kazemi, H., Fallah, Y., Nix, A. and Wayne, S. (2017) Predictive AECMS by Utilization of Intelligent Transportation Systems for Hybrid Electric Vehicle Powertrain Control. *IEEE Transactions on Intelligent Vehicles*, **2**, 75-84. https://doi.org/10.1109/TIV.2017.2716839

[6] eeNews Automotive (2012) Optimizing Performance and Fuel Economy of a Dual-Clutch Transmission Powertrain with Model-Based Design: Page 4 of 6. https://www.eenewsautomotive.com/content/optimizing-performance-and-fuel-economy-dual-clutch-transmission-powertrain-model-based/page/0/3

[7] Office of the Federal Register (2012) Code of Federal Regulations Title 40 Part 1066 Vehicle Testing Procedures. https://www.gpo.gov/fdsys/granule/CFR-2012-title40-vol34/CFR-2012-title40-vol34-part1066

[8] Office of the Federal Register (2011) Code of Federal Regulations Title 40 Part 1065 Engine Testing Procedures. https://www.govinfo.gov/app/details/CFR-2011-title40-vol33/CFR-2011-title40-vol33-part1065

[9] Center for Alternative Fuel Engines & Emissions (2018) Light-Duty Chassis Dynamometer. Morgantown.

[10] Society of Automotive Engineers International (2010) SAE J1711. https://www.sae.org/standards/content/j1711_201006/preview

[11] Transtronics Inc. (2017) Energy Density. https://xtronics.com/wiki/Energy_density.html

[12] Argonne National Laboratory (2011) Lower and Heating Values of Gas, Liquid, and Solid Fuels. Argonne.

[13] Cullen, K. (2007) DOE Biomass R&D TAC Meeting. https://biomassboard.gov/pdfs/cullen_vehicle_emission_interaction_with_low_and_high_concentration_ethanol_blend_fuelskw.pdf

[14] DeFries, T., Sabisch, M. and Kishan, S. (2014) In-Use Fuel Economy and CO_2 Emissions Measurement Using OBD Data on US Light-Duty Vehicles. *SAE International Journal of Engines*, **7**, 1382-1396. https://doi.org/10.4271/2014-01-1623

[15] George, D. (2018) Hybrid Electric Vehicle Torque Split Algorithms for Reduction of Engine Torque Transients. West Virginia University, Morgantown.

[16] Shen, W., Yu, H., Hu, Y. and Xi, J. (2016) Optimization of Shift Schedule for Hybrid Electric Vehicle with Automated Manual Transmission. http://www.mdpi.com/journal/energies

Appendix A: Shift Schedules

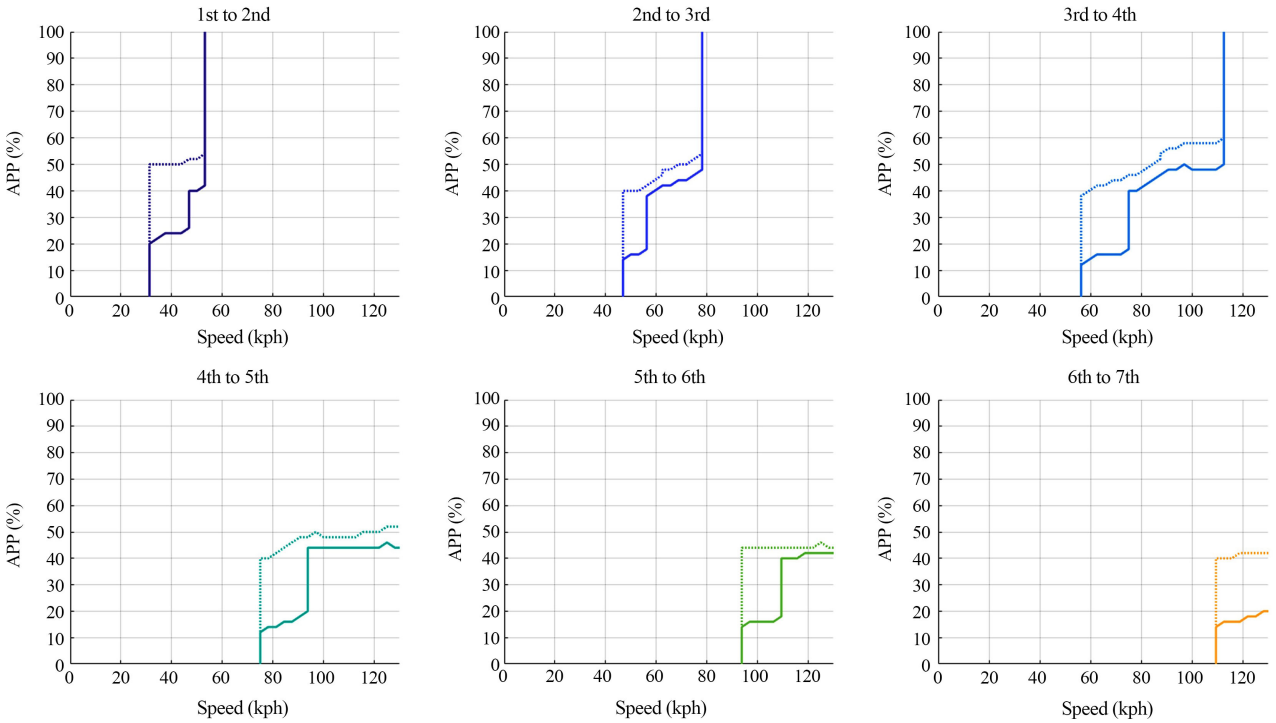

Figure A1. SOC dependent shift schedule upshift lines, target vs. 5% below target SOC. *Target SOC shift schedule indicated by dashed lines*, 5% *below target SOC indicated by solid lines.*

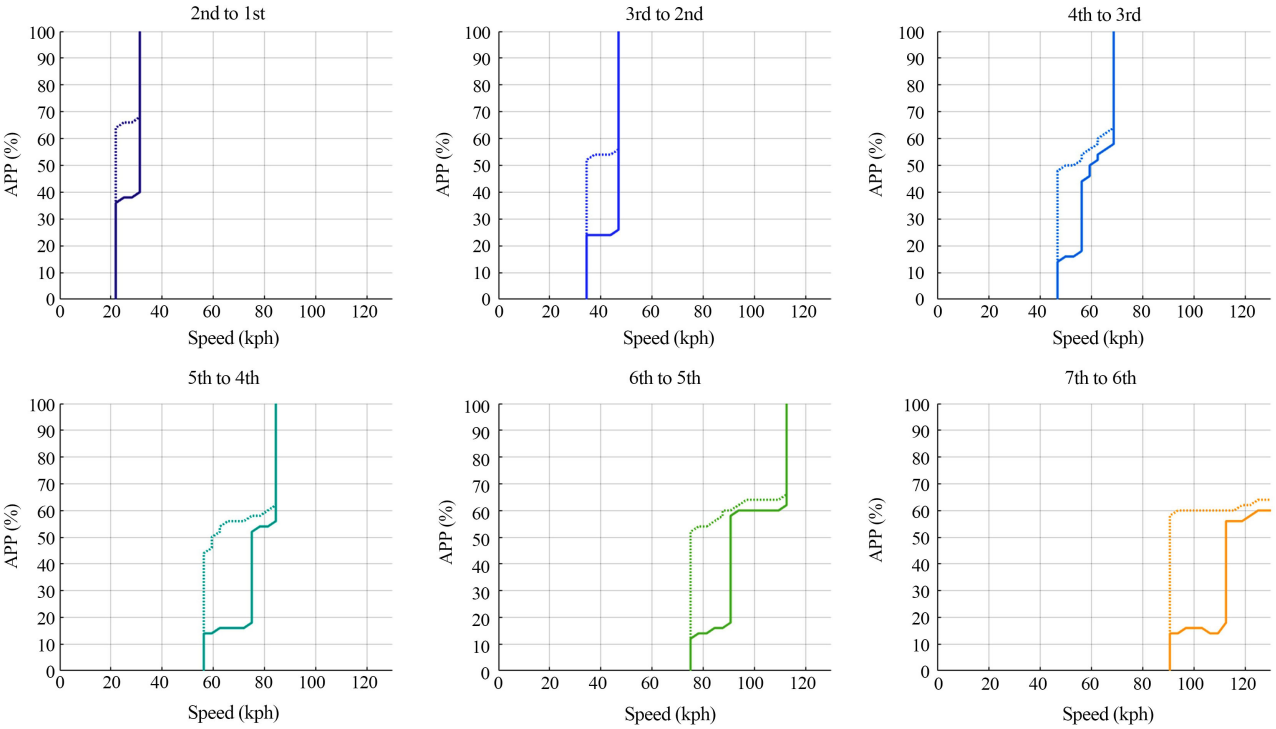

Figure A2. SOC dependent shift schedule downshift lines, target vs. 5% below target SOC. *Target SOC shift schedule indicated by dashed lines*, 5% *below target SOC indicated by solid lines.*

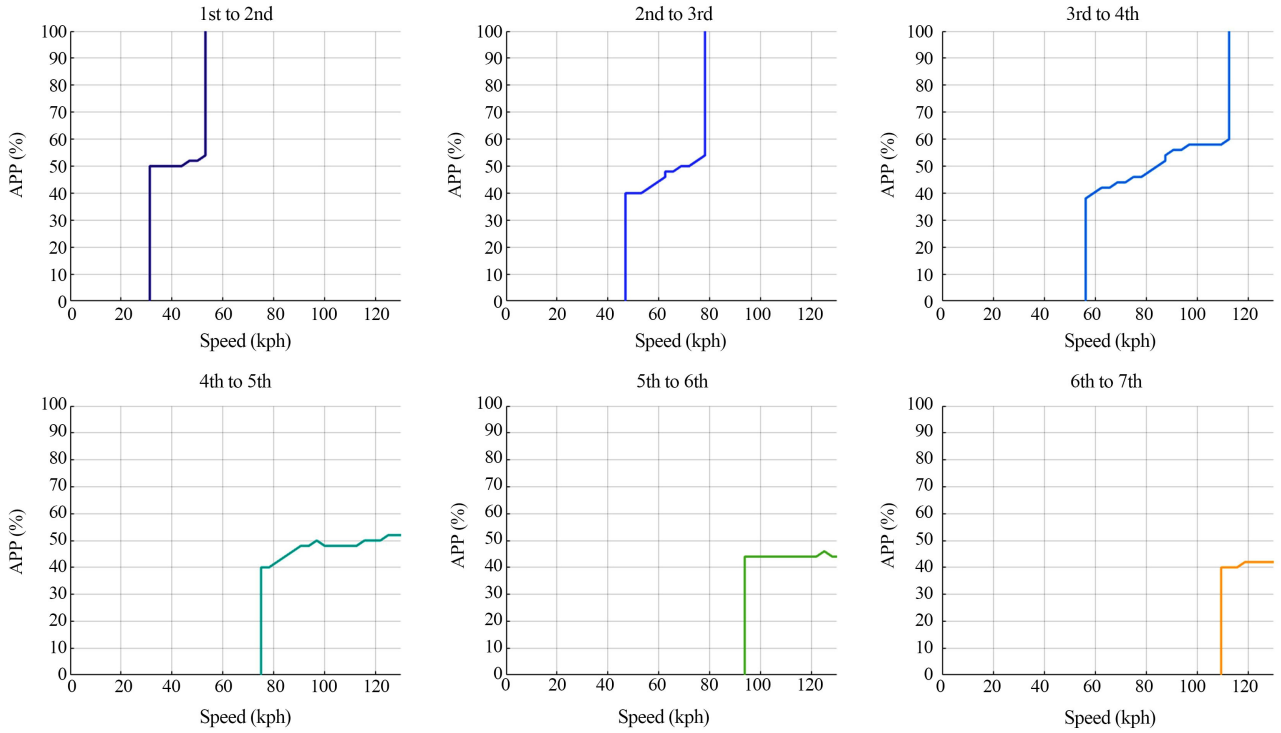

Figure A3. SOC dependent shift schedule upshift lines, target vs. 5% above target SOC. *Target SOC shift schedule indicated by dashed lines*, 5% *above target SOC indicated by solid lines. NOTE: In this case, no movement of the upshift lines was deemed necessary by the code.*

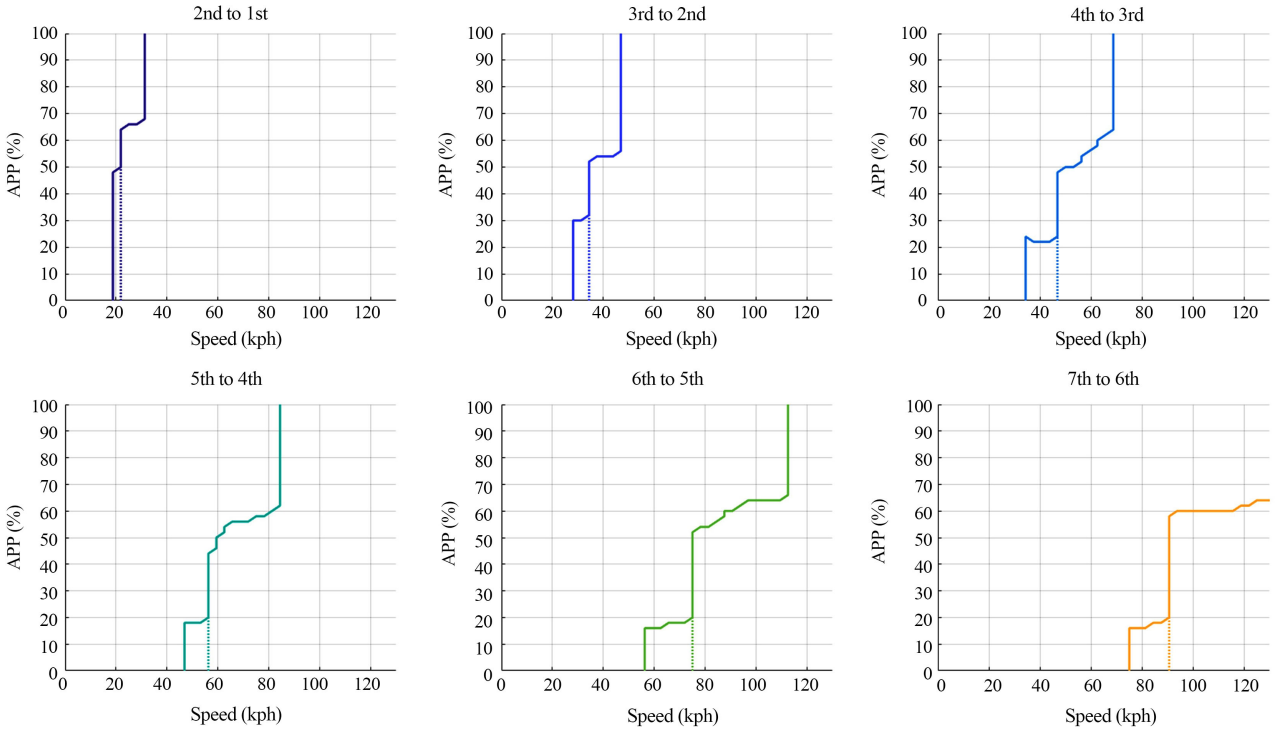

Figure A4. SOC dependent shift schedule downshift lines, target vs. 5% above target SOC. *Target SOC shift schedule indicated by dashed lines*, 5% *above target SOC indicated by solid lines.*

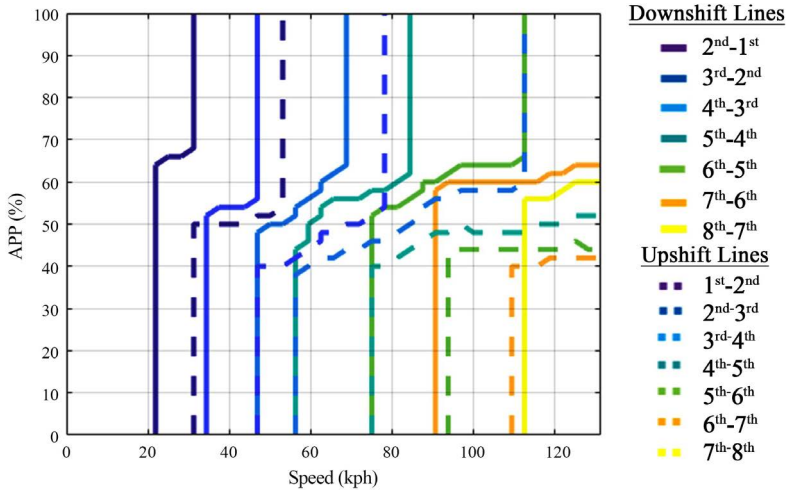

Figure A5. SOC independent shift schedule and shift schedule at target SOC of SOC dependent shift schedule.

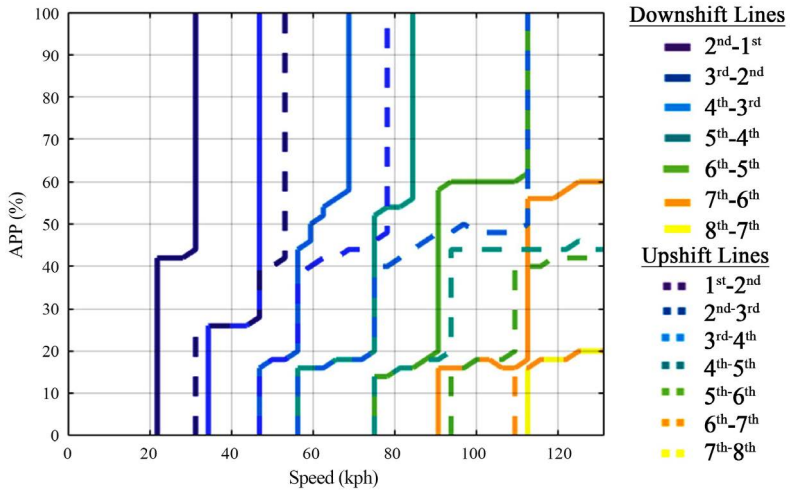

Figure A6. Shift schedule 1% below target SOC of SOC dependent shift schedule.

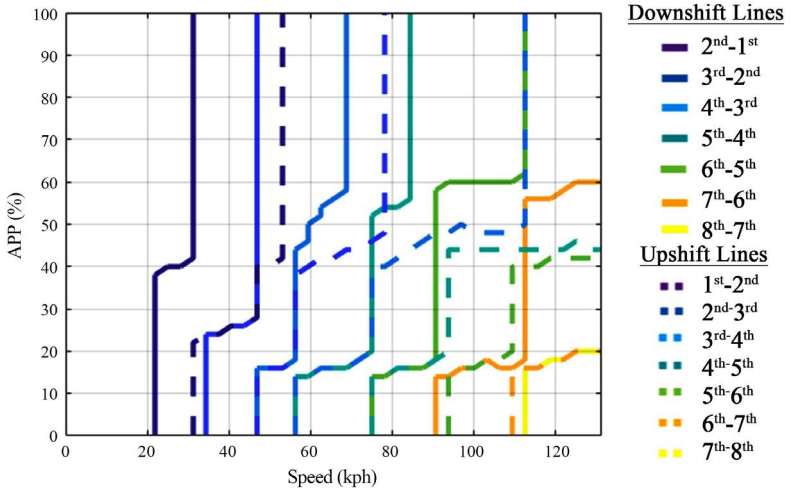

Figure A7. Shift schedule 3% below target SOC of SOC dependent shift schedule.

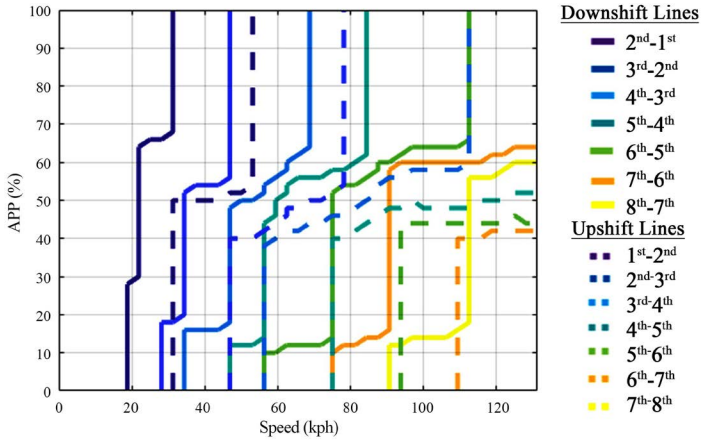

Figure A8. Shift schedule 1% above target SOC of SOC dependent shift schedule.

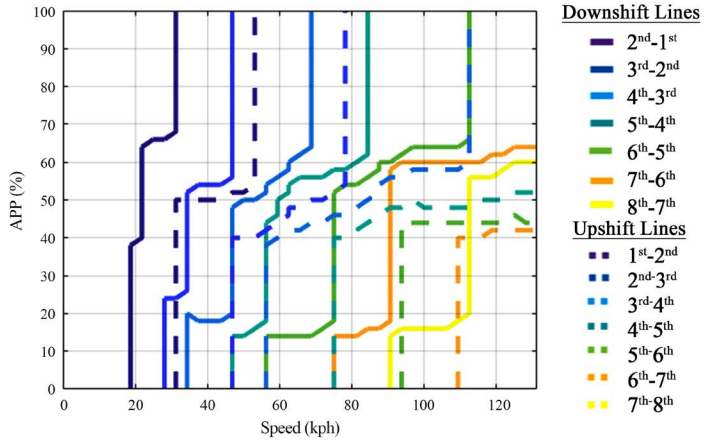

Figure A9. Shift schedule 3% above target SOC of SOC dependent shift schedule.

Appendix B: VIL Results

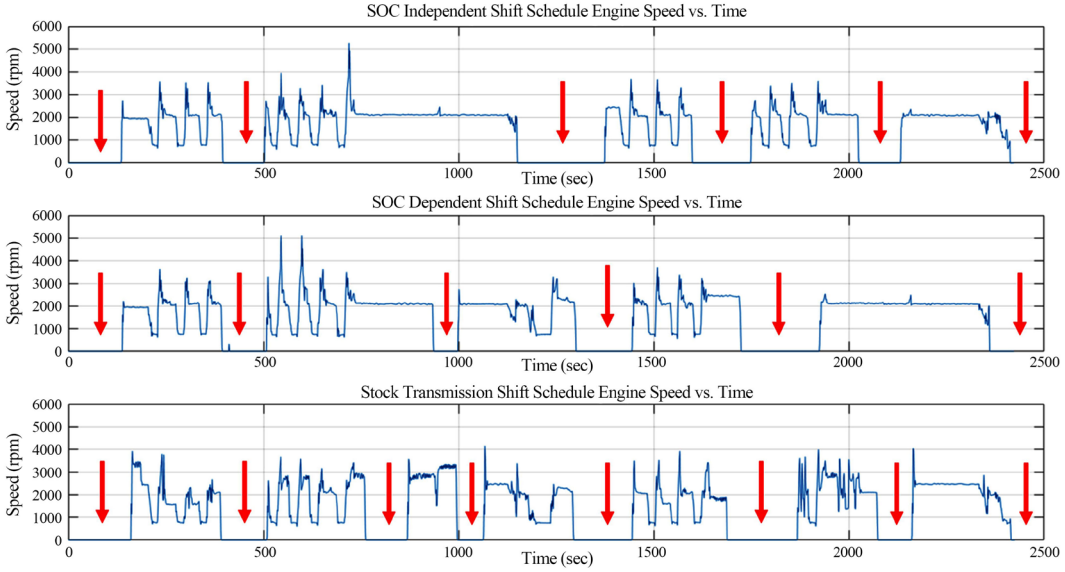

Figure B1. Engine shut-offs during VIL testing. *Engine shut-offs indicated by red arrow.*

Table B1. Total emissions and distance traveled during VIL testing.

Shift Schedule Used	Total Emissions (g)				Distance Traveled (mi)	
	CO	CO_2	HC	NOx	Engine On	Total
SOC Independent	18.1	8978.2	2.6	0.37	21.3	28.9
SOC Dependent	19.2	7736.2	2.8	0.09	21.9	28.8
Stock Transmission	31.8	8328.4	2.3	0.11	8.0	28.9

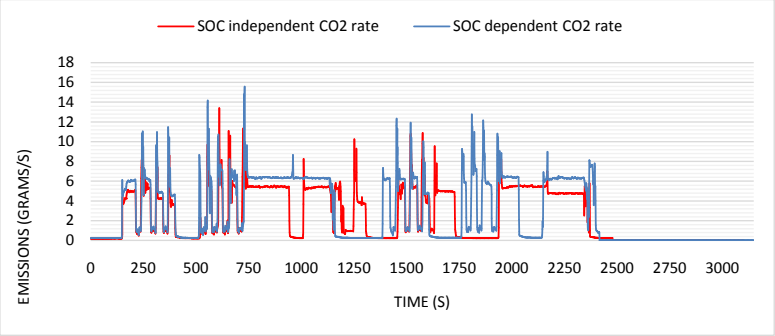

Figure B2. CO_2 emission rates of SOC independent and SOC dependent shift schedules.

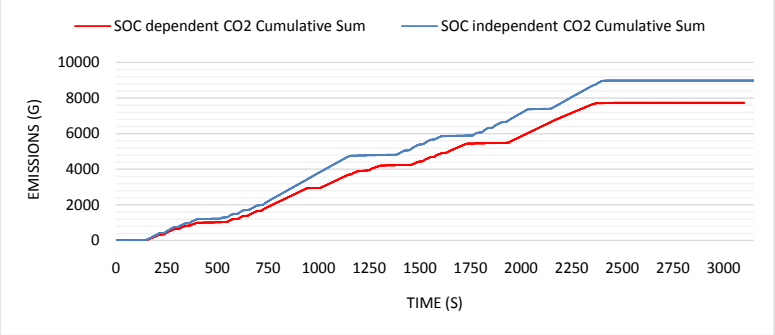

Figure B3. CO_2 emissions cumulative sum of SOC independent and SOC dependent shift schedules.

Appendix C: Sensitivity Analysis Results

Table C1. Sensitivity analysis of 5% below target summary table.

Parameter	Unit	Initial SOC of 35% (@ Target)	Initial SOC of 30% (5% < Target)	% Diff
Final SOC	%	36.5	36.7	+0.5%
Engine Fuel Economy [Equation (17)]	mpg	17.4	16.7	−4.2%
Engine Efficiency	%	28.7	28.9	+0.7%
Motor Discharge Efficiency	%	63.1	62.4	−1.1%
Motor Charge Efficiency	%	75.9	76.5	+0.8%
Vehicle Fuel Economy [Equation (16)]	mpgge	24.0	23.0	−4.4%
Vehicle Efficiency	%	38.0	38.7	+1.8%

Table C2. Sensitivity analysis of 5% above target summary table.

Parameter	Unit	Initial SOC of 35% (@ Target)	Initial SOC of 40% (5% > Target)	% Diff
Final SOC	%	36.5	36.5	0.0%
Engine Fuel Economy [Equation (17)]	mpg	17.4	18.2	+4.4%
Engine Efficiency	%	28.7	28.3	−1.4%
Motor Discharge Efficiency	%	63.1	64.4	+2.0%
Motor Charge Efficiency	%	75.9	74.4	−2.0%
Vehicle Fuel Economy [Equation (16)]	mpgge	24.0	25.1	+4.4%
Vehicle Efficiency	%	38.0	37.8	−0.5%

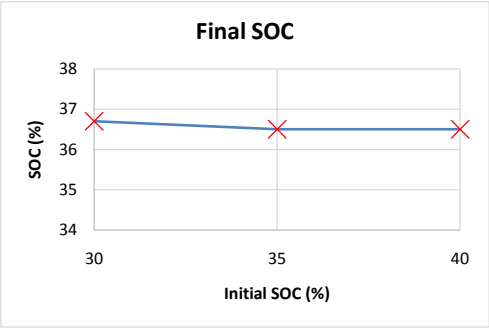

Figure C1. Final SOC vs. initial SOC of SOC dependent shift schedule.

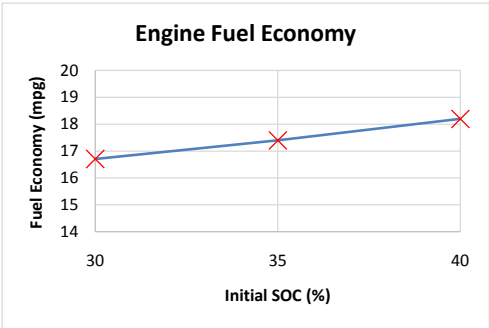

Figure C2. Engine fuel economy vs. initial SOC of SOC dependent shift schedule.

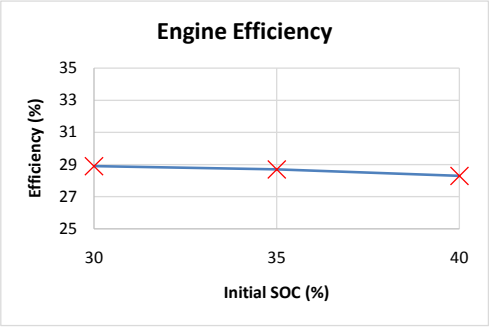

Figure C3. Average engine efficiency vs. initial SOC of SOC dependent shift schedule.

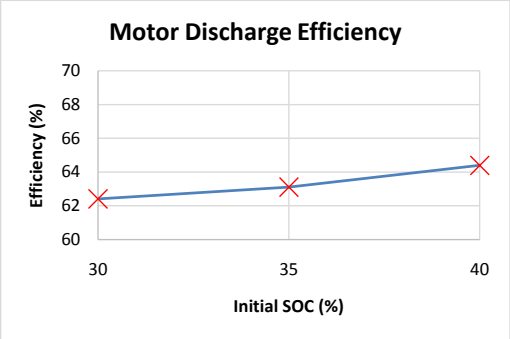

Figure C4. Average motor discharging efficiency vs. initial SOC of SOC dependent shift schedule.

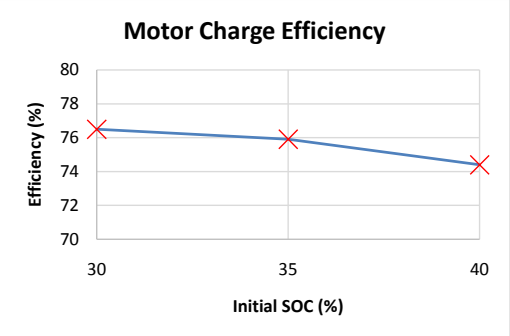

Figure C5. Average motor discharging efficiency vs. initial SOC of SOC dependent shift schedule.

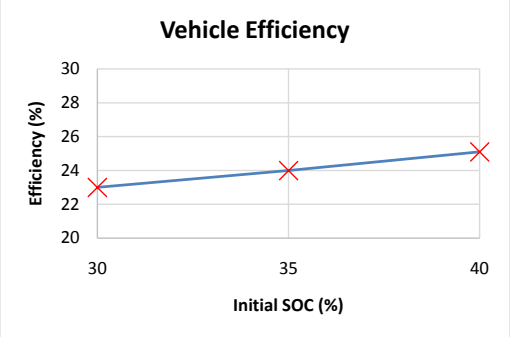

Figure C6. Vehicle fuel economy vs. initial SOC of SOC dependent shift schedule.